Interdiffusion and Composition Polydispersity in Diblock Copolymers above the Ordering Transition

T. Jian, S. H. Anastasiadis,*,† A. N. Semenov,‡ and G. Fytas*

Foundation for Research and Technology-Hellas, Institute of Electronic Structure and Laser, P.O. Box 1527, 71110 Heraklion Crete, Greece

G. Fleischer

Fakultät für Physik und Geowissenschaften, Universität Leipzig, D-04103 Leipzig, Germany

A. D. Vilesov

Institute of Macromolecular Compounds, Russian Academy of Sciences, 199004 St. Petersburg, Russia

Received September 26, 1994; Revised Manuscript Received December 27, 1994®

ABSTRACT: Photon correlation spectroscopy and pulsed-field-gradient nuclear magnetic resonance have been utilized in order to investigate the characteristic features of the recently established (both experimentally and theoretically) diffusive "polydispersity" relaxation process for concentration fluctuations in homogeneous diblock copolymer melts and solutions. This is accomplished using semidilute solutions of a symmetric mixture of two diblock copolymers with similar molecular weights and almost mirror compositions in a common good solvent. Mixing of the two asymmetric diblocks leads to a system with almost symmetric composition and with narrow molecular weight distribution, but with large effective composition polydispersity. Above the order to disorder transition (ODT), the theoretical expressions for the amplitude and the relaxation rate of the polydispersity mode can quantitatively describe the observed diffusive relaxation. Similarly to the situation in homopolymer blends, the thermodynamic forces can significantly retard the diffusion coefficient and lead to an increase in the dynamic intensity with increasing copolymer concentration. The intervention of the ODT alters this concentration dependence at copolymer concentrations ϕ near but below ϕ_{ODT}.

I. Introduction

Composition fluctuations are the key quantity in the description of the static[1] and dynamic[2] properties of diblock copolymers. In contrast to the polymer blends, the most prominent composition fluctuations $\psi_q(t)$ are short range with the relevant wavevector, q^*, at which the static structure factor attains its maximum value[3,4] satisfying the relation $q^*R_g = O(1)$, with R_g being the size of the copolymer chain. In fact, for monodisperse diblock copolymer melts, the long range $\psi_q(t)$ are suppressed and the mean field prediction[3] is a vanishingly small structure factor $S(q)$ for $q \ll q^*$.

The relaxation of ψ_q occurs[5,6] via a relative motion of the two blocks and, in the low q limit, the characteristic thermal decay rate is determined mainly by the terminal relaxation time. According to the random-phase approximation (RPA), this is the only mechanism for relaxing $\psi_q(t)$ in an incompressible, monodisperse diblock copolymer melt in the disordered state.[5,6] This internal relaxation mode has been experimentally observed both in the bulk[7,8] and in semidilute solutions in a common solvent.[9–11] For the latter, RPA predicts[6,12,13] an additional relaxation mode identified with the cooperative diffusion of the transient network of the overlapping polymer chains, observed experimentally as well.[10–12,14,15]

For disordered diblock copolymer melts[7,8,16,17] and semidilute copolymer solutions,[11,15,18–20] photon correlation spectroscopy (PCS) in the polarized geometry has revealed the presence of an additional diffusive relaxation identified[7,11,21] with the copolymer self-diffusion observable via the small but finite inherent composition polydispersity κ_o of the system. Due to the low and uncertain estimated values of κ_o ($\cong 10^{-2}$–10^{-3}) neither the proposed mechanism nor the applicability of the theoretical expression for the amplitude and dynamics of this process at low wavevectors has been critically examined.

In the present study, an investigation is presented on the characteristic features of this polydispersity mode by utilizing a symmetric mixture of two poly(styrene-*block*-butadiene) diblock copolymers with similar molecular weights and almost mirror compositions, f. Mixing of the two asymmetric diblocks leads to a system with almost symmetric composition and with very small molecular weight polydispersity, but with large effective composition polydispersity κ_o ($\cong 0.06$). Some preliminary experiments on this system have been presented recently.[22] The photon correlation spectroscopy measurements of the semidilute solutions in toluene (common solvent) are complemented by self-diffusion data obtained by pulsed-field-gradient nuclear magnetic resonance (PFG-NMR).[23] Above the order to disorder transition (ODT), the theoretical expressions for the amplitude and the relaxation rate of the polydispersity mode can quantitatively describe the experimental data for both the intensity and the diffusion coefficient of the observed relaxation. The thermodynamic forces can significantly retard the diffusion coefficient and lead to an increase in the dynamic intensity with increasing copolymer concentration. This large variation is significantly reduced by approaching the concentration ϕ_{ODT} at which the disorder to order transition (ODT) occurs at a given temperature.

* To whom correspondence should be addressed.
† Also at Physics Department, University of Crete, 711 10 Heraklion Crete, Greece.
‡ Permanent address: Physics Department, Moscow State University, 117234 Moscow, Russia.
® Abstract published in *Advance ACS Abstracts,* March 1, 1995.

0024-9297/95/2228-2439$09.00/0

This article is arranged as follows: In the Theoretical Background section (II), the current theoretical predictions for the relaxation modes of concentration fluctuations in diblock copolymer solutions are reviewed. Following the Experimental Section (III), the results of the polarized dynamic light scattering and PFG-NMR investigations are presented in section IV. In section V, the experimental data are discussed in relation to the predictions of the theory. Finally, the concluding remarks constitute section VII.

II. Theoretical Background

For homogeneous semidilute solutions of a monodisperse diblock copolymer in a nonselective good solvent, the random-phase approximation[6,12,13] predicts the existence of two relaxation modes for the dynamic structure factor of the effective polymer density fluctuations $g(q,t) = \langle \psi_q(t)\psi_{-q}(0)\rangle$, where $\psi(\mathbf{r}) = n_A{}^2\delta\phi_A(\mathbf{r}) + n_B{}^2\delta\phi_B(\mathbf{r})$ with n_K the refractive index of block K and $\delta\phi_K(\mathbf{r})$ the fluctuation of the volume concentration of the K component at a point $\mathbf{r}$. The first relaxation mode is the cooperative diffusion of the physical network formed by the overlapping chains, which is identical to that for semidilute homopolymer solutions.[24,25] The intensity I_{coop} and the diffusion coefficient, D_{coop}, of this process are given by

$$I_{coop} \propto (\bar{n}^{-2} - n_s{}^2)^2\phi^{-0.30}q^0 \tag{1a}$$

$$D_{coop} \propto \frac{k_BT}{6\pi\eta_s b}\phi^{0.77} \tag{1b}$$

where ϕ is the copolymer volume fraction, n_s and $\bar{n}$ are respectively the refractive index of the solvent and the average of the two blocks of the copolymer chain, η_s is the solvent shear viscosity, b is the statistical segment length, and q is the wavevector. The increase of D_{coop} with increasing ϕ is obeyed in the semidilute region, whereas in the concentrated regime D_{coop} decreases with copolymer volume fraction.

The second relaxation process concerns the relative motion of one block with respect to the other and is therefore a characteristic feature of the diblock copolymers. In the low-q limit, i.e., for $q^2R_g{}^2 \ll 1$, the internal mode is characterized by the intensity

$$I_{int} = (n_A{}^2 - n_B{}^2)^2\frac{1}{9}\phi^{0.77}vf^2(1-f)^2N^2b^2q^2 \tag{2a}$$

and the wavevector q-independent relaxation time

$$\tau_{int} \cong \tau_0 N^a\phi^b \tag{2b}$$

where N is the total number of segments in the copolymer chain, f is the volume fraction of segments of one type, v is the average segmental volume, n_K is the refractive index of block K of the diblock, $\tau_0 = \eta_s b^3/(k_BT)$ is the local jump time, and the exponents a and b take the appropriate values in the Rouse ($a = 2$, $b = 0.30$) and in the entanglement ($a = 3$, $b = 1.60$) regimes.[26] For a given N, large values of q and ϕ facilitate the experimental observation of the internal mode.

The existence of an additional diffusive relaxation process in the time correlation function of the light-scattering intensity from diblock copolymer melts[7,8,16,17] and solutions[11,18-20] has been very recently rationalized[7,11,21] in terms of the relaxation of the additional concentration fluctuations due to the composition polydispersity effects; these are inherent in all real systems and are shown[7,11,21] to relax via a diffusive mechanism of exchange of diblock chains of different composition. For disordered semidilute block copolymer solutions, the intensity, I_{poly}, and the diffusion coefficient, D, of this "polydispersity" mode are respectively given by[11]

$$I_{poly} = (n_A{}^2 - n_B{}^2)^2\frac{\kappa_o Nv\phi}{1 - 2\chi N\kappa_o\phi^{1.59}}q^0 \tag{3a}$$

and

$$D = D_s(N,\phi)\,(1 - 2\chi N\kappa_o\phi^{1.59}) \tag{3b}$$

where χ is the Flory–Huggins segment–segment interaction parameter, and $D_s(N,\phi)$ is the translational diffusion coefficient of the diblock chains in semidilute solutions (self-diffusion coefficient in the case of diblock copolymer melts[11,21]) that depends on concentration and molecular weight. In the Rouse regime, $D_s(N,\phi) \propto \phi^{-0.53}/N$, whereas in the entanglement regime, $D_s(N,\phi) \propto \phi^{-1.83}/N^2$. κ_o is a measure of the composition polydispersity of the diblock

$$\kappa_o = \frac{\langle N_A{}^2\rangle\langle N_B{}^2\rangle - \langle N_AN_B\rangle^2}{N^2\langle(N_A + N_B)^2\rangle} \tag{4}$$

where $N = \langle N_A + N_B\rangle$. Note that κ_o is sensitive to the composition polydispersity only; for a system of copolymer chains with the same composition, κ_o is equal to zero even if the distribution of total molecular weight is broad. It is worth mentioning the resemblance of eqs 3a and 3b with the interdiffusion process in polymer blends[5] and the necessity of a small but finite κ_o as well as moderate concentration ϕ for an experimental observation of the polydispersity process in diblock copolymer solutions.

A unique separation of all three relaxation processes in solution requires a careful adjustment of the experimental parameters, i.e., ϕ and q, as well as the sample characteristics, e.g. N, f, n_K's. In particular, the relevance of the thermodynamic effect in eqs 3a,b can be enhanced in the presence of large κ_o that increases further the contribution of the polydispersity mode in the dynamic light-scattering intensity. Experimental verification of the form of eqs 3a,b will allow the determination of the translational diffusivity of block copolymers by dynamic light scattering.

III. Experimental Section

Materials. Two poly(styrene-*block*-1,4-butadiene) diblock copolymers were prepared by anionic polymerization, as described before.[27] The diene microstructure was predominantly 1,4, and the molecular characteristics of the three copolymers are given in Table 1. Binary and ternary copolymer solutions in HPLC grade toluene solvent with polymer volume fraction $\phi \cong 0.05$ were prepared and filtered through a 0.22 μm Millipore filter into the dust-free light-scattering cell. In the symmetric ternary solution, the amount (by weight) of each copolymer was the same. During the measurements the cell was closed airtight to avoid evaporation of toluene. The concentration of all three solutions was gradually increased by slow evaporation of small amounts of solvent and determined by weighing the resulting solution. Photon correlation spectroscopy and PFG-NMR measurements were performed at 25 °C over a concentration range 1.5c^* to about 9c^*, with $c^* \cong 0.024$ g/cm^3 or 2.8 wt % the overlapping copolymer concentration. For the mixture of the two diblocks and by neglecting their inherent polydispersities, κ_o is esti-

Table 1. Sample Characteristics

species	M_n	M_w	M_w/M_n	w_{PS}[a]	N[b]	f_{PS}[c]	κ_o[d]	w_{ODT},[e] %
SB-1	68 100	73 600	1.08	0.228	956	0.200	5.9×10^{-3}	30–33
SB-2	69 400	72 200	1.04	0.735	891	0.700	6.1×10^{-3}	>24
mixture[f]				0.473	924	0.439	0.06	20–23

[a] Polystyrene weight fraction. [b] Based on average segmental volume. [c] Polystyrene volume fraction. [d] For the two diblocks, κ_o is estimated[11] by assuming independent molecular weight distributions of A and B blocks, i.e., as $\kappa_o \cong 2(M_w/M_n - 1)f^2(1-f)^2/[f^2 + (1-f)^2]$. [e] Weight percent at the ODT estimated from depolarized dynamic light scattering. [f] Values for w_{PS}, N, and f_{PS} for the mixture are estimations.

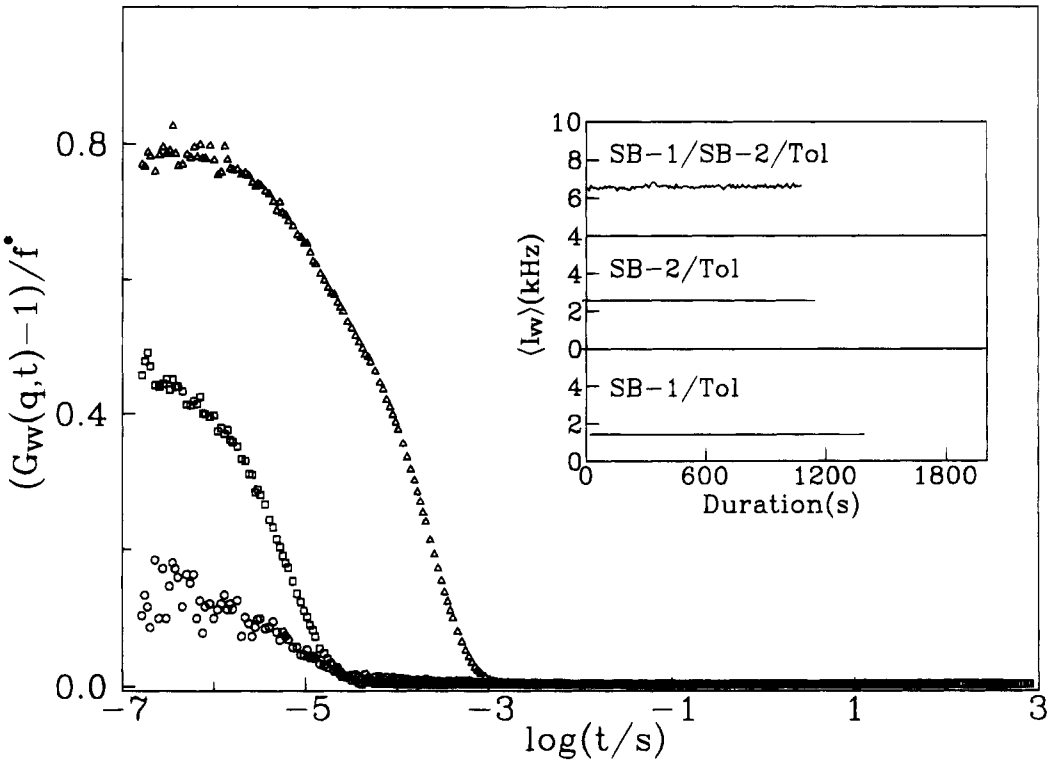

Figure 1. Experimental net intensity correlation function (eq 6) for the (○) binary SB-1/toluene (8.9 wt %), (□) binary SB-2/toluene (8.9 wt %), and (△) ternary SB-1/SB-2/toluene (9.3 wt %) solutions at 25 °C. The traces of the total light scattering intensity for the three solutions are given in the inset.

mated from eq 4 to be given by

$$\kappa_o = \frac{x_1 x_2 N_1^2 N_2^2}{(x_1 N_1 + x_2 N_2)^2 (x_1 N_1^2 + x_2 N_2^2)} (f_1 - f_2)^2 \qquad (5)$$

where x_i is the number fraction of chains of diblock i with molecular weight M_i and fraction of block A f_i. x_i is related to the weight fractions by $x_i = (w_i/M_i)/\Sigma(w_i/M_i)$. For the present mixture of equal weight fractions of the two diblocks in Table 1, κ_o(mixture) = 0.06, i.e., 10 times larger than the one calculated for the individual diblocks (Table 1).

Photon Correlation Spectroscopy (PCS). The autocorrelation function of the polarized light-scattering intensity, $G_{VV}(q,t) = \langle I_{VV}(q,t)\, I_{VV}(q,0)\rangle / \langle |I_{VV}(q,0)|^2\rangle$, with $I_{VV}(q,0)$ the mean light-scattering intensity, is measured at different scattering angles, θ, using an ALV spectrophotometer and an ALV-5000 full digital correlator over the time range 10^{-7}–10^3 s. Both the incident beam from an Adlas diode-pumped Nd-YAG laser, with wavelength λ = 532 nm and single mode intensity 160 mW, and the scattering beam were polarized perpendicular (V) to the scattering plane. $q = (4\pi n/\lambda)\sin(\theta/2)$ is the magnitude of the scattering vector, with n the refractive index of the medium. In quasi-elastic light scattering under homodyne conditions, $G_{VV}(q,t)$ is related to the desired normalized field correlation

$$G_{VV}(q,t) = [1 + f^* |a\, g(q,t)|^2] \qquad (6)$$

where f^* is an experimental factor calculated by means of a standard, and a is the fraction of $\langle I_{VV}(q,0)|\rangle$ with decay times slower than about 10^{-7} s.

Figure 1 shows experimental net correlation functions for the two binary SB-1/toluene (8.9 wt %) and SB-2/toluene (8.9 wt %) and the ternary SB-1/SB-2/toluene (9.3 wt %) semidilute solutions at q = 0.025 nm^{-1} and 25 °C. The trace of the intensity $I_{VV}(q)$ for the three solutions during the accumulation time is shown in the insets.

The experimental correlation functions, $g(q,t)$ are often represented by the Kohlrausch–Williams–Watts function, $g(q,t) = \exp[(-(t/\tau)^\beta]$, where τ and $\beta \le 1$ are respectively the relaxation time and shape parameter. $\beta = 1$ corresponds to single exponential relaxational modes usually observed for diffusive processes. For multiple relaxation processes, the experimental correlation functions may be analyzed by performing the inverse Laplace transform (ILT) of $g(q,t)$, without assumption of the shape of the distribution function $L(\ln \tau)$ but by assuming as a superposition of exponentials:

$$a g(q,t) = \int_{-\infty}^{\infty} L(\ln \tau) \exp(-t/\tau)\, d(\ln \tau) \qquad (7)$$

This determines a continuous spectrum of relaxation times $L(\ln \tau)$; the average times obtained from $L(\ln \tau)$ are used to determine the characteristic relaxation times.

Pulsed-Field-Gradient NMR (PFG-NMR). The basis of the technique is a stimulated echo measurement using the proton spin as a probe; it measures the translational diffusion coefficient D_s of particles bearing ^{1}H nuclei, if the field gradient is applied as a pulse during the spin-echo experiment.[28] A magnetic gradient pulse of amplitude g is applied for a

dephasing period δ and the echo amplitude $\Psi(k^2t)$ is measured during the time interval, t, between the field gradient pulses. The amplitude of the generalized wavevector is defined as $k = \gamma g\delta$, with γ being the gyromagnetic ratio and g and δ the height and the width of the field gradient pulses. The generalized wavevector may be varied via either the gradient amplitude g or the pulse duration δ. However, switching the gradient on and off does not permit the reduction of δ below about 10^{-3} s. Large k values require strong magnetic field gradients and are limited by thermal and mechanical problems with the large currents in the field gradient coil. The range of k in the present experiments extends to about 8.5×10^{-4} Å^{-1}. The longest accessible diffusion times, on the other hand, are determined by the spin–lattice relaxation time T_1 on the order of seconds; t may be varied between 10^{-3} s and T_1.

The echo amplitude $\Psi(k^2t)$ of the binary copolymer solutions is well represented by a single exponential decay function yielding the chain diffusivity $D_s(N,\phi)$. In the case of the copolymer mixture, however, $\Psi(k^2t)$ is better described by a double exponential function with a fixed contribution of each copolymer. The two translational diffusivities are by a factor of 2 apart over the examined concentration range and rather characterize the individual copolymer components of the symmetric mixture. Figure 2 shows that the normalized spin-echo experimental data for the SB-1/toluene and the SB-1/SB-2/toluene solutions with 20 wt % polymer conform to a single and a double exponential representation, respectively. The fact that the data obtained for various diffusion times between 30 and 300 ms superimpose indicates normal diffusion with mean-squared displacement $\langle r^2\rangle \propto t$.

IV. Results

A single relaxation process contributes to the experimental correlation functions of the solutions of both SB-1 and SB-2 samples in toluene for $\phi < 0.1$, as indicated in Figure 1. This process is the cooperative diffusion of the entangled network that displays a lower intensity for the SB-1/toluene solution. For this sample rich in butadiene, the average refractive index, $\bar{n}$, is closer to the refractive index of the solvent, n_s, than for the SB-2 copolymer rich in styrene. In fact the experimental ratio between the intensity $a_{coop}I_{VV}$ associated with the cooperative diffusion in the two samples is reproduced by the contrast factor $(\bar{n}^2 - n_s^2)^2$ in these samples. Here, a_{coop} is the amplitude of the cooperative diffusion process obtained from the ILT analysis (eq 7) of the experimental correlation function and I_{VV} is the polarized scattering intensity normalized to that of toluene. In the symmetric ternary mixture of Figure 1, this relaxation mode displays intensity intermediate between those of the binary solutions although the total scattering intensity is much higher; the additional intensity relaxes with a slower process evident in the experimental $G(q,t)$ that is associated with the mutual diffusion due to the large composition polydispersity (see below). The latter process is also present in the $G(q,t)$ of the parent copolymer solutions at higher concentrations.

Figure 3 displays experimental intensity correlation functions at 25 °C for a 20.1 wt % SB-2/toluene solution at two different scattering angles, $\theta = 45$ and 150°, and for a 20.7 wt % SB-1/SB-2/toluene solution at $\theta = 150°$. The distribution of relaxation times obtained by the ILT analysis multiplied by the normalized total scattering intensity is shown in the insets of Figure 3 for both solutions. At the highest wavevector, i.e., highest scattering angle, the shape and amplitude of $I_{VV}L(\log \tau)$ for the two solutions is very different. In the ternary solution, there is one main contribution at $\tau \cong 3 \times 10^{-3}$ s and a hint of a second faster peak at $\tau \cong 3 \times 10^{-6}$ s, whereas the weighted distribution functions for the binary solution exhibit a three-peak structure. The peaks at $\tau \cong 3 \times 10^{-6}$ s and $\tau \cong 10^{-3}$ s are attributed, respectively, to the cooperative and "polydispersity" mode since both have a q^2-dependent rate and q-independent amplitude (see upper inset in Figure 3 and ref 11). Moreover, the amplitude of the second diffusive process increases by almost 2 orders of magnitude in the ternary solution which was prepared in order to have large composition polydispersity (see Table 1). In fact, the fast cooperative diffusion mode can barely be resolved due to the large contribution of the "polydispersity" mode.

The intermediate peak at $\tau \cong 3 \times 10^{-5}$ s in the SB-2/toluene system exhibits an amplitude that depends on q and a q-independent relaxation rate; both findings are in accordance with the characteristics of the internal relaxation mode of eq 2 (see also ref 11). Thus, at $\theta = 45°$, i.e., at low wavevector q, the internal relaxation peak is overwhelmed by the cooperative diffusion process. As is also evident from eq 2, the relaxational characteristics of the internal chain motion can be revealed at high q's for a high degree of polymerization N and for a relatively large copolymer concentration.

The diffusive character of the main relaxation process in the SB-1/SB-2/toluene system is shown in Figure 4a for a total copolymer concentration of 9.3 wt %. The virtually q-independent total amplitude of the experimental $G(q,t)$, short time intercept ~0.8, also reflected in the distribution of relaxation times (upper inset of Figure 4a) along with the insensitivity of the total light-scattering intensity to wavevector variations in the low-q limit, supports the theoretical predictions (eqs 1a and 3a) for the polydispersity and the cooperative diffusion modes. Note that about 90% ($\sqrt{0.8}$) of the total intensity is relaxing by these two processes and about 80% is associated with the slower polydispersity mode for the 9.3 wt % solution at 25 °C. The relaxation rate $\Gamma = 1/\tau$ obtained from the most probable τ, at which $L(\ln \tau)$ attains its maximum value, is proportional to q^2 for both processes (lower inset of Figure 4a). An increase of the copolymer concentration at constant q improves the resolution since both the intensity and the relaxation rates of the two modes turn out to exhibit opposite concentration dependences (eqs 1 and 3). In fact, the insets in Figure 4b illustrate the merging of the two dynamics at low copolymer concentrations; increasing copolymer concentration results in an enhancement and a slowing down of the slow process in contrast to the reduction and speed-up of the cooperative diffusion mode. The opposite concentration trend of the dynamics is depicted in the second inset of Figure 4b, whereas for comparison reasons, we have plotted the bare $L(\ln \tau)$ and not $I_{VV}(\log \tau)$ in the first inset; a plot of the latter would significantly suppress the fast peak.

In conclusion, the experimental results for the ternary diblock copolymer system with large effective composition polydispersity unambiguously show that the slow diffusive mode is of the same origin as that in almost monodisperse diblock copolymer solutions. The strong concentration dependence of the relaxational characteristics of this relaxation mode will be discussed in terms of the theoretical expressions eqs 3a and 3b in the next section.

V. Discussion

Interdiffusion. Close inspection of Figure 3 reveals that the slow diffusive process gains enormously in amplitude and becomes slower in the ternary SB-1/SB-

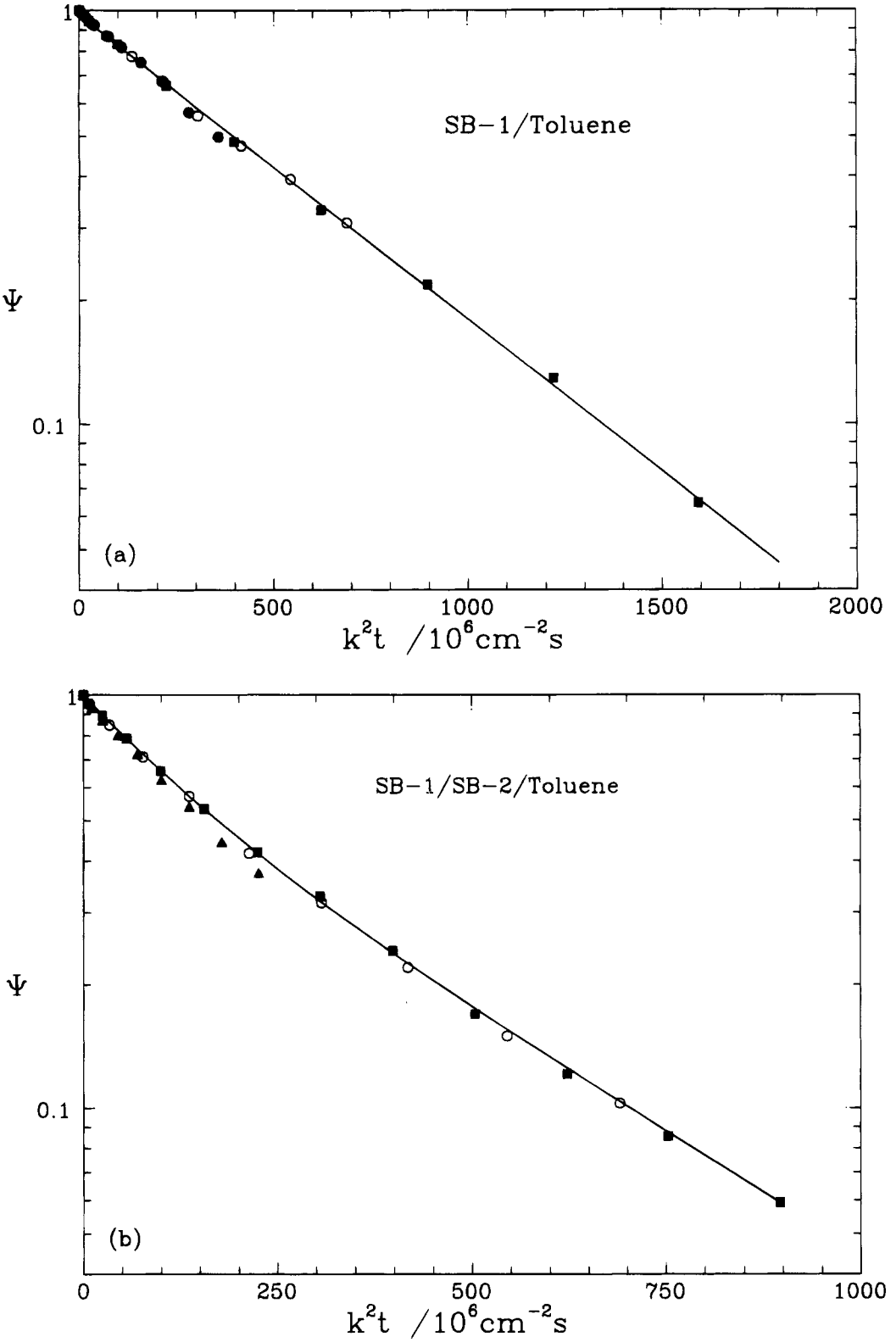

Figure 2. Spin-echo amplitude for (a) SB-1/toluene (20 wt %) and (b) SB-1/SB-2/toluene (20 wt %) solutions at 25 °C as measured with PFG-NMR versus the product of the square of the effective scattering vector, k, and the time, t. Data are shown for various diffusion times; t = 54 ms (●), 104 ms (○), 304 ms (■), and 34 ms (▲). The straight line in (a) denotes a single exponential decay whereas the line in (b) is a fit to the data for t = 304 ms and indicates a double exponential representation.

2/toluene system (large effective composition polydispersity κ_0 in Table 1) relative to that in the binary SB-2/toluene solution (low κ_0). Based on eq 3b, the diffusion coefficient, D, of the latter should assume values very close to the translational diffusion coefficient D_s of the SB-2 chains in the solution; at $\phi = 0.15$, and 25 °C, eq 3b with the assumption $\chi = 0.1$ results in $D/D_s \cong 0.95$. On the contrary, this ratio reduces to 0.42 for the ternary system at $\phi = 0.15$ due to the larger influence of the composition polydispersity term. Increase of the concentration ϕ will enhance the thermodynamic interactions ($\propto \chi N\phi^{1.59}$ in eq 3), retarding further the collective diffusion coefficient. This theoretically anticipated behavior is experimentally documented.

Figure 5 shows the variation of the diffusion coefficients with polymer volume fraction at 25 °C for both

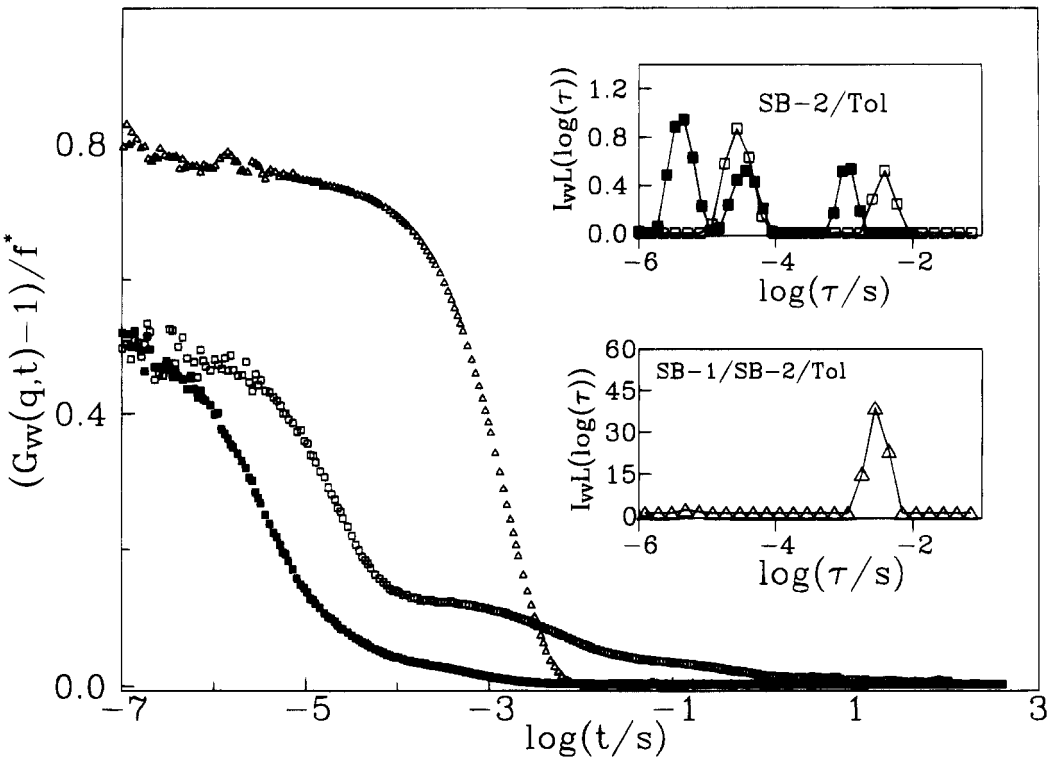

Figure 3. Experimental net intensity correlation functions at 25 °C for a 20.1 wt % binary SB-2/toluene solution at two scattering angles $\theta = 45°$ (□) and 150° (■) and a 20.7 wt % ternary SB-1/SB-2/toluene solution at $\theta = 150°$ (△). The distributions of relaxation times obtained from the ILT analysis (eq 7) weighted by the total light scattering intensity normalized to the intensity of toluene are shown in the insets. Both solutions have very similar total copolymer volume fractions $\phi \cong 0.19$.

the SB-1/toluene and the ternary SB-1/SB-2/toluene solution. As expected, the cooperative diffusion coefficient D_{coop}, characterizing the concerted motion of the network relative to the solvent, is an increasing function of ϕ and assumes experimentally identical values in the two systems (eq 1b). The data apparently reveal the predicted scaling behavior for homopolymers in the semidilute regime and agree quantitatively with data for semidilute polystyrene homopolymer solutions.[11,40] The translational diffusion coefficient $D_s(N,\phi)$ of a polymer chain in semidilute solutions, on the other hand, is a decreasing function of ϕ (arising from the reduction of the number of links g per blob[11,22-24]) and scales with $\phi^{-0.53}/N$ in the Rouse and $\phi^{-1.83}/N^2$ in the entanglement regime. The concentration dependence of the experimental translational diffusion coefficients, $D_s(N,\phi)$, for the diblock copolymer chains obtained from PFG-NMR (also shown in Figure 5) exceeds the predicted scaling behavior of $\phi^{-1.83}$ for the entanglement regime in good solvents. This deviation probably arises from the solution crossing from the semidilute to the concentrated regime at concentrations[24-26] around 0.2, where it is the concentration dependent friction coefficient that affects the diffusion coefficient. Besides, as will be discussed later, the systems are neither well in the Rouse nor well in the reptation regime. In agreement with eq 3b, the interdiffusion coefficient D, obtained from PCS, for SB-1/toluene agrees within experimental error with the translational diffusion coefficient D_s, obtained from NMR. This agreement extends up to concentrations near the ϕ_{ODT}. One can therefore employ PCS to measure chain diffusion of almost monodisperse diblock copolymers taking advantage of the very small but finite inherent composition polydispersity.

For the composition polydisperse ternary system, the closeness between the experimental D and $D_s(N,\phi)$ is restricted only to the lowest concentration ϕ. Since the concentration dependence of purely kinetic origin is captured in the $D_s(N,\phi)$, the observed decrease of $D/D_s(N,\phi)$ is likely due to the thermodynamic interactions expressed in the term in parentheses in eq 3b. An experimental verification of the concentration dependence of this term is attempted in the plot of Figure 6. The quantity $\phi N/I_{poly}$ should be virtually independent of the copolymer concentration if the term $2\chi N\kappa_o$ is much less than 1. This is the case for SB-1, as indicated in Figure 6a in agreement with the closeness between the values of D and D_s in this system (Figure 5). On the contrary, the I_{poly} for the ternary system with large effective κ_o displays a stronger concentration dependence and hence $\phi N/I_{poly}$ is found to decrease with ϕ. According to eq 3a, $\phi N/I_{poly}$ should vary linearly with $\phi^{1.59}$, which is shown in Figure 6a. A similar linear dependence is predicted (eq 3b) and approximately found (Figure 6b) for D/D_s on $\phi^{1.59}$. Both sets of data conform to a linear fit for $\phi < 0.15 < \phi_{ODT}$ yielding $2\chi N\kappa_o = 12 \pm 1$ at 25 °C, which for the N and κ_o values of the present system results in interaction parameter χ values (0.1 ± 0.01) similar to the ones in the literature between polystyrene and polybutadiene.

The concurrent deviation of the data from the behavior predicted by eqs 3a and 3b at higher concentrations near the ODT but still in the disordered state (see also Figure 6c, where the data are plotted according to a manipulation of eqs 3a and 3b) suggests that the rate of the slowing down of D and the increase of I_{poly} is reduced simultaneously, deviating from the expressions in eqs 3a and 3b. A few possible explanations may be suggested to explain this deviation. The growth of the long wavelength ($q \rightarrow 0$) concentration fluctuations expected near the macrophase separation which may be induced by the composition polydispersity, that would correspond to a divergence of I_{poly}, eq 3a, is apparently

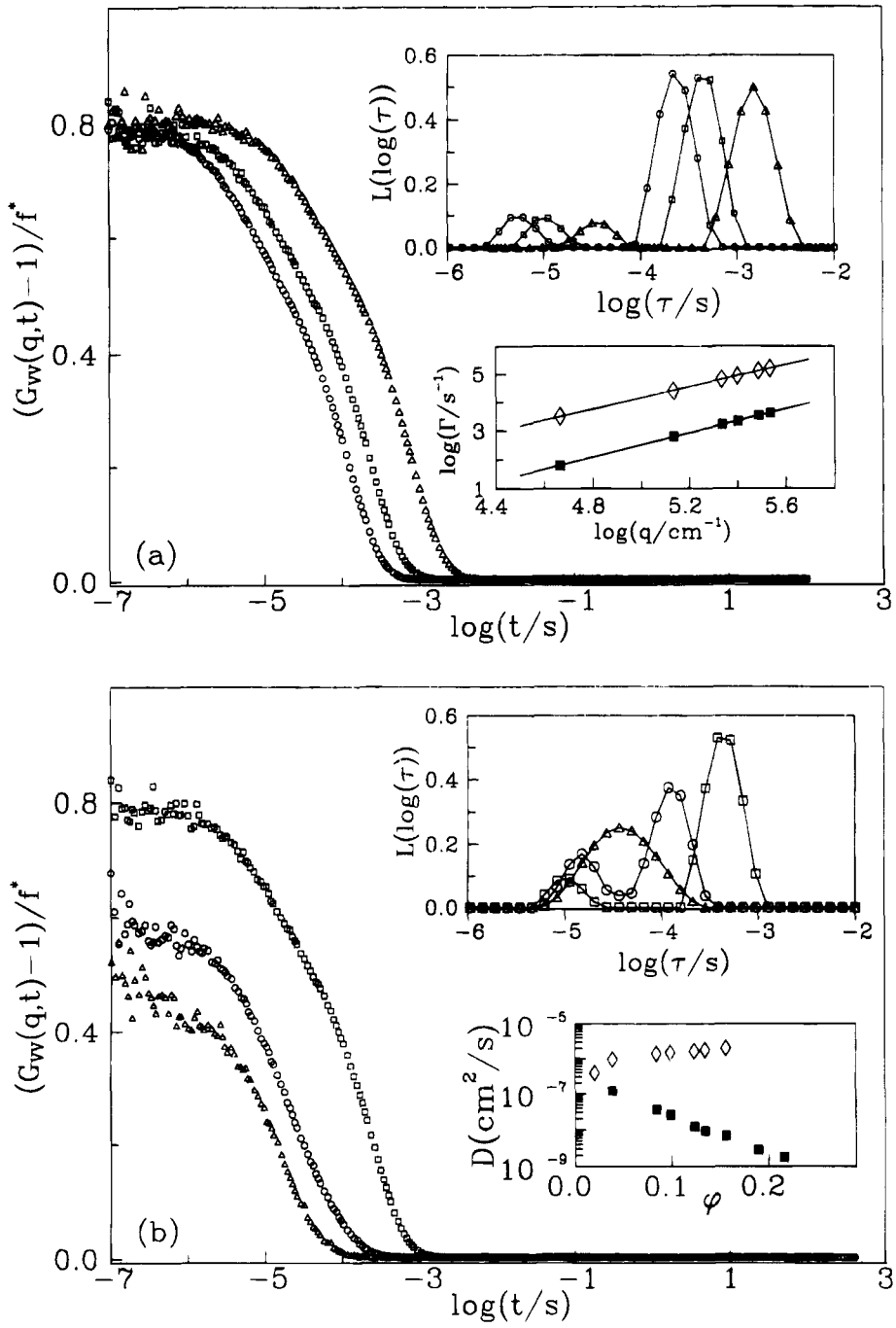

Figure 4. (a) Experimental net intensity correlation functions for a 9.3 wt % SB-1/SB-2/toluene solution at $\theta = 45°$ (△), 90° (□), and 150° (○). The corresponding bimodal distribution relaxation functions and the variation of the relaxation rates for the cooperative (◇) and the polydispersity (■) modes with the wavevector q are shown in the insets. (b) Variation of the net intensity correlation function for SB-1/SB-2/toluene solutions with copolymer concentrations 2.3 (△), 4.3 (○), and 9.3 wt % (□). The respective distribution relaxation functions are shown in the upper inset, whereas the variation of the diffusion coefficients for the cooperative (◇) and the polydispersity (■) modes with copolymer concentration are shown in the lower.

reduced via intervention of a microphase separation of the copolymer solution. Indeed, depolarized dynamic light scattering[11,31] showed that, at 25 °C, the ternary system undergoes a disorder to order transition between 20 and 23 wt %, i.e., at $\phi_{ODT} \cong 0.20 \pm 0.01$. At the same time composition fluctuation effects[4] may influence the scattering from the diblock copolymer solution[29] even for the low wavevectors of light scattering, especially in view of the decrease in the characteristic wavevector of the most prominent composition fluctuations with an increase in the polydispersity.[30] Another possibility is that the $\phi^{1.59}$ scaling dependence of the blob–blob effective interaction parameter (eqs 24–26 in ref 11) is valid in semidilute solutions but for $\phi \ll 1$. For larger ϕ's, one can anticipate some corrections to this scaling law. The fact, however, that the combination $DI_{poly}/(\phi N D_s)$ in Figure 6c is not constant near the ODT is interesting and is currently under investigation.

Discussing the possibility of a competition between macrophase and microphase separation in the present ternary system, one should consider that the stability limit for macrophase separation will correspond to concentration ϕ_{macro} where $1 - 2\chi N\kappa_o\phi_{macro}^{1.59} = 0$, whereas microphase separation takes place at $\phi_{ODT} \cong 0.20 \pm 0.01$, as discussed above. Using the previous result $2\chi N\kappa_o = 12 \pm 1$ at 25 °C, ϕ_{macro} is estimated to be 0.21 ± 0.01. Therefore, ϕ_{macro} is only slightly higher than ϕ_{ODT}, and the interplay between micro- and mac-

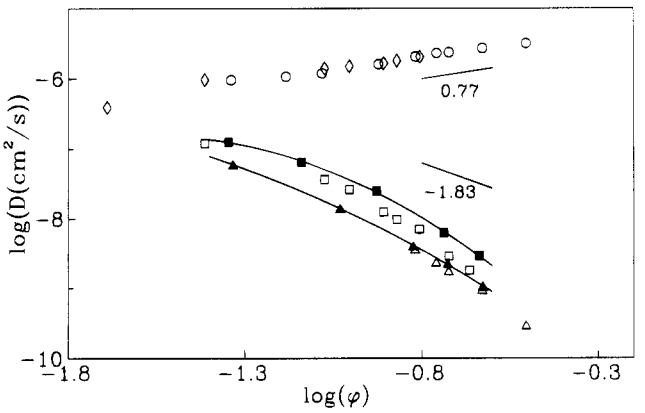

Figure 5. Concentration dependence of the cooperative diffusion (○, ◇), interdiffusion (△, □), and translational diffusion (▲, ■) in SB-1/toluene (○, △, ▲) and SB-1/SB-2/toluene (◇, □, ■) solutions at 25 °C. The slopes +0.77 and −1.83 are the predictions for semidilute solutions for the cooperative and the translational diffusivities in the entanglement regime, respectively. The solid lines through the translational diffusion coefficients are to guide the eye.

rophase separation might be important. Also note that the above estimate of ϕ_{macro} is strictly valid for wavevector $q = 0$; for the finite light scattering q's, a negative correction to the estimated ϕ_{macro} must be included. Macrophase separation was not observed experimentally in the present system even at higher concentrations, indicating that the development of the ordered morphology prevents the macrophase separation.

Summarizing, the predictions for the existence and the behavior of the new diffusive relaxation termed polydispersity mode for diblock copolymers in melt and in solution are quantitatively verified in a system where the effective composition polydispersity was enhanced using the ternary system of two copolymers of almost equal N but different compositions in a common solvent. Possible explanations for the deviations of the predicted behavior near the ODT were discussed.

Translational Diffusivity. The disparity between the translational diffusion, D_s, values for the ternary system and binary SB-1/toluene especially at higher concentrations (Figure 5) is a hint of a larger difference between the translational diffusivities of the two asymmetric copolymer chains SB-1 and SB-2 in toluene. The transport coefficients obtained by PFG-NMR are shown in Figure 7 for the two binary solutions and the ternary solution at various concentrations measured at 25 °C. The error bars shown in Figure 7 for the translational diffusion coefficients obtained for the ternary system correspond to the analysis of the experimental response function $\Psi(k^2t)$ of the PFG-NMR by a double exponential function (see also Figure 2b), resulting in two effective diffusivities characteristic of the two kinds of copolymer chains in the ternary solution. Note that due to the fact that dynamic light scattering measures the collective diffusive process, i.e., the interdiffusion, the average diffusivities obtained by the well-accepted "fast mode ansatz" for highly mobile polymer blends[32] were used in the previous discussion relative to Figures 5 and 6.

The differences in the translational diffusivities of the two parent diblock copolymers should be discussed. For example, at 20 wt % copolymer, the D_s of the SB-2 sample rich in styrene is larger by a factor of about 8 than the D_s of the SB-1 system rich in the more mobile butadiene; bulk polystyrene has much higher glass transition temperature T_g (~373 K) than bulk 1,4-polybutadiene (~183 K). This factor of 8 cannot be explained by the slightly different N's (Table 1) and the small difference in the volume fractions corresponding to the same copolymer weight percent, due to the different densities.

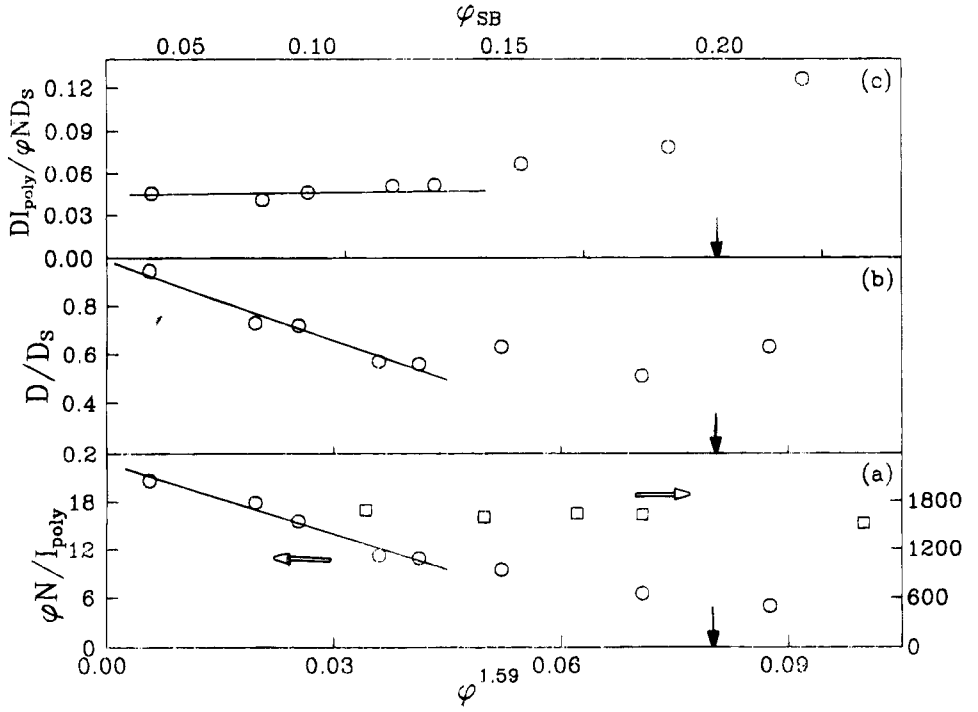

Figure 6. Intensity I_{poly} associated with the composition polydispersity (a) and the ratio D/D_s (b) of the interdiffusion to the chain diffusivity plotted versus polymer volume fraction for SB-1/SB-2/toluene solutions (○), as implied by eq 3. The solid lines represent linear least squares fits (see text). The upper part, (c), shows a combination of the two plots (a, b) also dictated by eq 3. For comparison, the intensity I_{poly} in SB-1/toluene (□) is shown also in (a). The black arrows denote the region of the ODT for the ternary system.

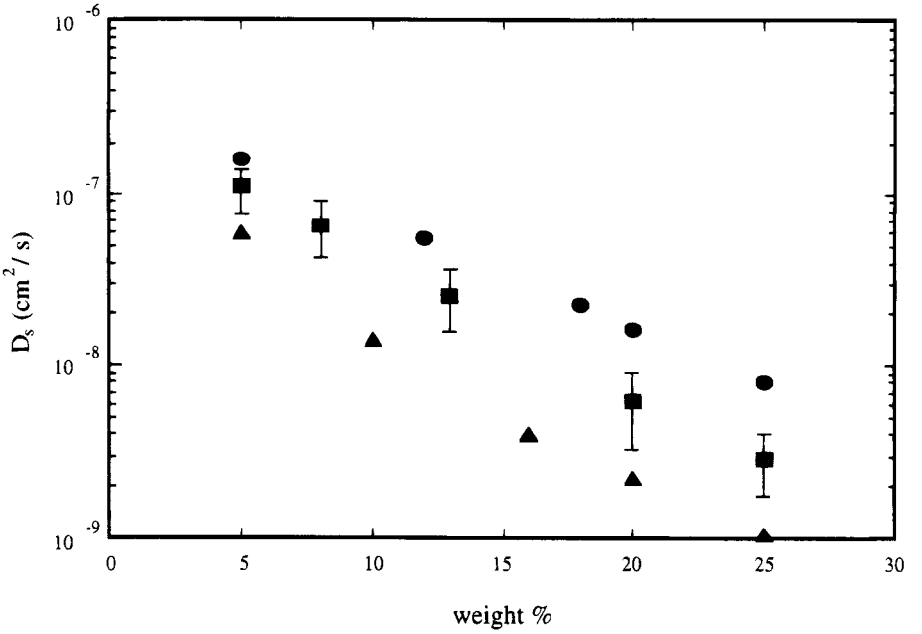

Figure 7. Translational diffusivities in the two binary SB-1/toluene (▲) and SB-2/toluene (●) solutions and the ternary SB-1/SB-2/toluene (■) solution obtained from PFG-NMR at different copolymer volume fractions at 25 °C. See text for the error bars for the diffusivities for the ternary solution.

Table 2. Entanglement Characteristics

species	M_c	N_c[a]	N_e[b]	ϕ_e[c]	ϕ_c[d]	w_c[e]
polystyrene	35 000	394	179			
polybutadiene	4 500	71	32			
SB-1			41	0.043	0.094	0.099
SB-2			90	0.101	0.222	0.248
SB-1/SB-2			57	0.062	0.137	0.148

[a] Based on average segmental volume. [b] $N_e \cong N_c/2.2$.[33] [c] $\phi_e \cong N_e/N$. [d] $\phi_c \cong 2.2\phi_e$. [e] Weight fractions corresponding to the volume fractions ϕ_c.

This difference will be attributed below to the different entanglement densities in the three solutions. Theory for the translational diffusivities for semidilute homopolymer solutions predicts[24-26] that for chains obeying Rouse dynamics, the self-diffusivity scales as $D_s(N,\phi) \propto k_BT\phi^{-0.53}/(\eta_s bN)$, whereas in the entanglement regime $D_s(N,\phi) \propto k_BT\phi^{-1.83}/(\eta_s bN^2)$. The characteristic number of segments between entanglements in solution, $N_e(\phi)$ is related to that in the bulk, N_e, by[33] $N_e(\phi) \cong N_e\phi^{1-\alpha}$, where α is a universal constant for similar ranges of interaction densities and $\alpha = 2$; thus $N_e(\phi) \cong N_e\phi^{-1}$. Therefore, there is a characteristic concentration, $\phi_e \cong N_e/N$, and a respective critical concentration for entanglements, $\phi_c \cong 2.2\,\phi_e$, above which the polymer chains are entangled. The above expressions show that the polymer properties get involved in the expressions for the diffusivities via only the N_e values, which do not explicitly interfere in the calculations but determine the Rouse and the reptation regimes. The glass transition temperature of the polymer, on the other hand, that affects significantly the mobility in the bulk state does not appear in the expressions, and it is the solvent viscosity that controls the mobility whereas the blob size results in the explicit ϕ dependence. In contrast, for concentrated solutions or the bulk state, it is the friction coefficients and, therefore, the solution or bulk viscosities that control the mobility.

The critical molecular weights for entanglements, M_c, for bulk polystyrene and polybutadiene are vastly different[33] and are listed in Table 2 together with the values for N_c, the critical number of segments for reptation, calculated using the average segmental volume, and the calculated N_e values. In order to calculate N_e for the diblock copolymers, the mixing rule proposed for the plateau modulus of a polymer blend[34,35] is adopted, which leads to the following expression for the number of segments between entanglements for the diblock

$$(N_e)_{\text{diblock}}^{-1} = [f(N_e)_A^{-1/2} + (1-f)(N_e)_B^{-1/2}]^2 \quad (8)$$

The values for the resulting N_e, ϕ_e, ϕ_c, and the respective weight fractions w_c are also shown in Table 2. The calculations for the critical weight fractions for reptation show that SB-1 will be entangled already above 10 wt %, whereas SB-2 only above 25 wt % and the mixture above 15 wt %. This means that in the larger part of the concentration range of the translational diffusion measurements, SB-1 is probably obeying the reptation dynamics whereas SB-2 is closer to exhibiting Rouse behavior and the blend is somewhere in between. This qualitatively explains the trend for the magnitude of the measured diffusivities. It should be noted, however, that the crossover between the Rouse and the reptation regime is rather broad[36] and, in the melt, well-entangled behavior is observed only for molecular weights greater than about $5M_c$.[36] Therefore, one cannot assume that even the solutions with the highest concentrations are well-entangled in order to obey the $\phi^{-1.83}/N^2$ scaling, which makes quantitative comparison of the data for the two diblocks almost impossible. Moreover, there is a difference of a factor of about 2.5 between the diffusivities for the two diblocks even at concentrations (5 wt %) where both systems should obey Rouse dynamics. This disparity cannot be explained by either the previous discussion or by the slight difference between the N's of the two diblocks; this apparent dependence of the translational diffusivity in solution on the diblock composition is currently under investigation.[37]

Another point that should be mentioned is the insensitivity of the translational diffusion coefficient for the ternary system to the crossing of the ODT. Depolarized dynamic light-scattering measurements show that the ternary solution undergoes a disorder to order transition

in the concentration regime between 20 and 23 wt %. A flat featureless correlation function is observed at 20 wt % (as well as at all lower concentrations), corresponding to the disordered state, whereas a relaxation process appears in the window of the correlator for the 23 wt % solution accompanied by a significant increase in the depolarized intensity, in agreement with previous investigations.[11,31] The depolarized scattering again is due to the establishment of significant form anisotropy due to grains of coherently ordered lamellae in the ordered state with correlation length of the $O(\mu m)$. Mixing two cylinder-forming asymmetric poly(styrene-*b*-butadiene) copolymers of molecular weights smaller than of the diblocks here in order to get a symmetric system in the melt resulted in a mixture exhibiting lamellae ordering, as verified by small-angle X-ray scattering and transmission electron microscopy and in agreement with Monte-Carlo computer simulations.[38] Therefore, lamellae structure is expected when our ternary system crosses the ODT. The translational diffusion data for the ternary system in Figure 7 show a smooth concentration dependence between 20 and the 25 wt % that conforms with the smooth variation of the temperature dependence of the self-diffusion and tracer-diffusion data measured by PFG-NMR and forced Rayleigh scattering, respectively, on poly(styrene-*block*-isoprene)[23,39] and poly(ethylenepropylene-*block*-ethylethylene)[40] diblock copolymers in the bulk; this was attributed to concentration fluctuation effects[4,41] that retard chain mobility even at temperatures well above the ODT, especially for entangled diblocks.

VI. Concluding Remarks

Photon correlation spectroscopy and pulsed-field-gradient nuclear magnetic resonance measurements were used in order to investigate the characteristic features of the newly observed diffusive relaxation process in disordered diblock copolymer systems in melts and semidilute solutions. Recent theoretical predictions attributed the process to the relaxation of the additional long-wavelength concentration fluctuations in homogeneous diblocks originating from the inherent composition polydispersity of the system. The diffusion coefficient was predicted to be controlled by the translational diffusion coefficient of the diblock copolymer chains. Utilizing a series of semidilute solutions in a common good solvent of a symmetric mixture of two poly(styrene-*b*-butadiene) diblock copolymers with similar molecular weights and almost mirror compositions, i.e., a system with almost symmetric composition, very small molecular weight polydispersity, but large effective composition polydispersity (κ_0), it was shown that the experimental data for both the intensity and the diffusion coefficient of the observed relaxation can be quantitatively accounted for by the theoretical expressions for the amplitude and the relaxation rate of the polydispersity diffusive mode. The thermodynamic forces, expressed as $\chi N\kappa_0\phi^{1.59}$, can significantly retard the diffusion coefficient and lead to an increase in the dynamic intensity with increasing copolymer concentration, when κ_0 is large enough. For anionically synthesized diblock copolymers, κ_0 is usually of the $O(10^{-2}-10^{-3})$ and, thus, the diffusion coefficient of the process is the self-diffusion of the copolymer chains. The dependence of the translational diffusion coefficients of diblock copolymer chains in semidilute solutions on diblock composition, f, was discussed; the different critical molecular weights for entanglements of the two species were found to be very important in determining the diffusion coefficients. Besides, the insensitivity of the translational diffusion coefficient to the crossing of the ODT was once more shown.

Acknowledgment. We would like to thank Dr. E. Melenevskaya of the Institute of Macromolecular Compounds, Russian Academy of Sciences, St. Petersburg, Russia, for synthesizing and providing the diblock copolymers used in this work. A.N.S. acknowledges the hospitality and financial support of the Foundation for Research and Technology-Hellas. S.H.A. would like to acknowledge that part of this research was sponsored by NATO's Scientific Affairs Division in the framework of the Science for Stability Programme and by the Greek General Secretariat of Research and Technology. G. Fytas acknowledges the financial support of the Alexander von Humboldt Foundation (Grant No. FOKOOP USS 1685). G. Fleischer acknowledges financial support from the Deutsche Forschungsgemeinschaft (SFB 294).

References and Notes

(1) Bates, F. S.; Fredrickson, G. H. *Annu. Rev. Phys. Chem.* **1990**, *41*, 525. Bates, F. S. *Science* **1991**, *251*, 898.
(2) Fytas, G.; Anastasiadis, S. H. In *Disorder Effects on Relaxation Processes*; Richert, R., Blumen, A., Eds.; Spinger Verlag: Berlin, 1994; p 697.
(3) Leibler, L. *Macromolecules* **1980**, *13*, 1602.
(4) Fredrickson, G. H.; Helfand, E. *J. Chem. Phys.* **1987**, *87*, 697.
(5) Akcasu, A. Z.; Benmouna, M.; Benoit, H. *Polymer* **1986**, *27*, 1935. Akcasu, A. Z.; Tombakoglu, M. *Macromolecules* **1990**, *23*, 607. Akcasu, A. Z. *Macromolecules* **1991**, *24*, 2109.
(6) Borsali, R.; Vilgis, T. A. *J. Chem. Phys.* **1990**, *93*, 3610.
(7) Anastasiadis, S. H.; Fytas, G.; Vogt, S.; Fischer, E. W. *Phys. Rev. Lett.* **1993**, *70*, 2415.
(8) Vogt, S.; Anastasiadis, S. H.; Fytas, G.; Fischer, E. W. *Macromolecules* **1994**, *27*, 4335.
(9) Borsali, R.; Benoit, H.; Legrand, J.-F.; Duval, M.; Picot, C.; Benmouna, M.; Farago, B. *Macromolecules* **1989**, *22*, 4119. Duval, M.; Picot, C.; Benoit, H.; Borsali, R.; Benmouna, M.; Lartigue, C. *Macromolecules* **1991**, *24*, 3185.
(10) Duval, M.; Haida, H.; Lingelser, J. P.; Gallot, Y. *Macromolecules* **1991**, *24*, 6867.
(11) Jian, T.; Anastasiadis, S. H.; Semenov, A. N.; Fytas, G.; Adachi, K.; Kotaka, T. *Macromolecules* **1994**, *27*, 4762.
(12) Borsali, R.; Fischer, E. W.; Benmouna, M. *Phys. Rev. A* **1991**, *43*, 5732.
(13) Benmouna, M.; Benoit, H.; Borsali, R.; Duval, M. *Macromolecules* **1987**, *20*, 2620.
(14) Haida, H.; Lingelser, J. P.; Gallot, Y.; Duval, M. *Die Makromol. Chem.* **1991**, *192*, 2701.
(15) Konák, C.; Podesva, J. *Macromolecules* **1991**, *24*, 6502. Konák, C.; Vlcek, P.; Bansil, R. *Macromolecules* **1993**, *26*, 3717.
(16) Anastasiadis, S. H.; Fytas, G.; Vogt, S.; Gerharz, B.; Fischer, E. W. *Europhys. Lett.* **1993**, *22*, 619.
(17) Vogt, S.; Jian, T.; Anastasiadis, S. H.; Fytas, G.; Fischer, E. W. *Macromolecules* **1993**, *26*, 3357.
(18) Balsara, N. P.; Stepanek, P.; Lodge, T. P.; Tirrell, M. *Macromolecules* **1991**, *24*, 6227.
(19) Tsunashima, Y.; Kawamata, Y. *Macromolecules* **1994**, *27*, 1799.
(20) Pan, C.; Maurer, W.; Liu, Z.; Lodge, T. P.; Stepanek, P.; von Meerwall, E. D.; Watanabe, H. *Macromolecules*, submitted for publication.
(21) (a) Fytas, G.; Anastasiadis, S. H.; Semenov, A. N. *Makromol. Chem., Macromol. Symp.* **1994**, *79*, 117. (b) Semenov, A. N.; Fytas, G.; Anastasiadis, S. H. *Polym. Prepr.* **1994**, *35* (1), 618.
(22) Jian, T.; Fytas, G.; Anastasiadis, S. H.; Vilesov, A. D. *Polym. Mater. Sci. Eng.* **1994**, *71*, 767.
(23) Fleischer, G.; Fujara, F.; Stühn, B. *Macromolecules* **1993**, *26*, 2340.
(24) Doi, M.; Edwards, S. F. *The Theory of Polymer Dynamics*; Oxford Science Publishers: Oxford, U.K., 1986.
(25) Schaefer, D. W.; Han, C. C. In *Dynamic Light Scattering*; Pecora, R., Ed.; Plenum Press: New York, 1985.
(26) de Gennes, P. G. *Scaling Concepts* in *Polymer Physics*; Cornell University Press: Ithaca, NY, 1979.
(27) Nesterov, V. V.; Kurenbin, D. I.; Krasikov, V. D.; Beleukii, B. G. *Talanta* **1987**, *34*, 161.

(28) Kärger, J.; Pfeifer, H.; Heink, W. *Adv. Magn. Reson.* **1988**, *12*, 1.
(29) Fredrickson, G. H.; Leibler, L. *Macromolecules* **1989**, *22*, 1238.
(30) Burger, C.; Ruland, W.; Semenov, A. N. *Macromolecules* **1990**, *23*, 3339.
(31) Jian, T.; Anastasiadis, S. H.; Fytas, G.; Adachi, K.; Kotaka, T. *Macromolecules* **1993**, *26*, 4706.
(32) Meier, G.; Fytas, G.; Momper, B.; Fleischer, G. *Macromolecules* **1993**, *26*, 5310 and references therein. Jordan, E. A.; Ball, R. C.; Donald, A. M.; Fetters, L. J.; Jones, R. A. L.; Klein, J. *Macromolecules* **1988**, *21*, 235. Composto, R. J.; Kramer, E. J.; White, D. M. *Macromolecules* **1988**, *21*, 2580. Kanetakis, J.; Fytas, G. *Macromolecules* **1989**, *22*, 3452. Sillescu, H. *Makromol. Chem., Rapid Commun.* **1984**, *5*, 519; **1987**, *8*, 393.
(33) Graessley, W. W.; Edwards, S. F. *Polymer* **1981**, *22*, 1329.
(34) Tsenoglou, C. *J. Polym. Sci., Polym. Phys. Ed.* **1988**, *26*, 2329. Tsenoglou, C. In *New Trends in the Physics and Chemistry of polymers*; Lee, L.-H., Ed.; Plenum Press: New York, 1989.
(35) Composto, R. J.; Mayer, J. W.; Kramer, E. J.; White, D. M. *Polymer* **1990**, *31*, 2320. Composto, R. J.; Kramer, E. J.; White, D. M. *Macromolecules* **1992**, *25*, 4167.
(36) Ferry, J. D. *Viscoelastic Properties of Polymers*; Wiley: New York, 1970.
(37) Anastasiadis, S. H.; Fleischer, G.; Adachi, K.; Kotaka, T. Manuscript in preparation.
(38) Vilesov, A. D.; Floudas, G.; Pakula, T.; Melenevskaya, E. Yu.; Birshtein, T. M.; Lyatskaya, Yu. V. *Makromol. Chem.* **1995**, in press.
(39) Ehlich, D.; Takenaka, M.; Hashimoto, T. *Macromolecules* **1993**, *26*, 492.
(40) Dalvi, M. C.; Eastman, C. E.; Lodge, T. P. *Phys. Rev. Lett.* **1993**, *71*, 2591. Dalvi, M. C.; Lodge, T. P. *Macromolecules* **1994**, *27*, 3487.
(41) Bates, F. S.; Rosedale, J. H.; Fredrickson, G. H. *J. Chem. Phys.* **1990**, *92*, 6255.

MA945033B